DYNAMIC MONITORING FOR EARLY FAILURE DIAGNOSIS AND MODERN TECHNIQUES FOR DESIGN OF POSITIVE DISPLACEMENT PUMPING SYSTEMS

by

Faustino Martinez

Mechanical Reliability Engineer

DuPont Ibérica, S.A.

Asturias, Spain

Martin Philippin

Mechanical Engineer

LEWA Herbert Ott GmbH

Leonberg, Germany

James M. Blanding

Consultant and Technology Leader

E.I. DuPont de Nemours & Company, Inc.

Houston, Texas

and

Eberhard Schlücker

Head of Engineering

LEWA Herbert Ott GmbH

Leonberg, Germany

Faustino Martinez is an Industrial Engineer with DuPont Ibérica, S.A., in Asturias, Spain. Since joining DuPont in 1993, he has had broad responsibility for mechanical reliability in the THF plant, which produces feedstock for Lycra™. Through this work Mr. Martinez has developed significant expertise with centrifugal compressors and other large rotating machinery components and systems as well as with high-pressure process diaphragm pumps, online dynamic monitoring systems, and the fields of mechanical vibration and fluid pulsation. Prior work experience includes the Iberdrola Power Company and the Ceasa Pulping Mill, both in Asturias, Spain.

Mr. Martinez graduated from the University of Oviedo-Escuela Técnica Superior de Ingenieros Industriales de Gijón (1991).

Martin Philippin is a Mechanical Engineer in the Service Department of LEWA Herbert Ott GmbH, in Leonberg, Germany. He joined Lewa in 1996 as a Service-Engineer, responsible for triplex process diaphragm pumps.

After finishing his apprenticeship in Mechanical Technology, Mr. Philippin studied Mechanical Engineering, which included one year of study in the United States, and obtained his Dipl.-Ing. degree at Konstanz Technical University.

James M. Blanding is Consultant and Technology Leader for the Process Equipment Group in Engineering at the DuPont Company, in Houston, Texas. Joining DuPont in 1981, he consults generally in dynamic analysis of fluid and structural systems. He is responsible for all technology and software tools, both internal and third-party, used in DuPont for process fluid transient and dynamic analysis. Particular areas of emphasis include analyses of performance and pulsation of reciprocating compressors and positive displacement pumps, fluid/structural/control system dynamic modeling, design of agitated reactor internals, and dynamic measurements and monitoring.

Dr. Blanding received his B.S. and M.S. degrees (Mechanical Engineering) from Virginia Tech before joining Union Carbide in 1976 as a consultant in acoustics. He returned to Virginia Tech in 1978 where he served three years as Instructor on the Faculty of Mechanical Engineering and earned his Ph.D. degree.

ABSTRACT

Competitive marketplace pressures for higher quality products with consistent material properties at lower cost are changing the face of chemical process manufacturing facilities. More frequently today, critical equipment is installed in unspared service with minimal onsite spare parts, yet demanded to operate reliably without defects for greater periods of time. An important component that helps make this possible is the emergence of increasingly more powerful and lower cost online condition monitoring systems for early failure diagnosis.

These systems have moved into the relatively inhospitable chemical plant environment, capability that until recently was largely the domain of the engineering laboratory. High-frequency dynamic measurement, with automated statistical and mathematical post-processing, is now available live, remotely, via the Internet across the globe. This paper examines this technology in applications with several high-pressure process diaphragm pumping systems. Many key learnings are explored along with advances in system design that have been developed as a result of application of these techniques.

Numerous real examples illustrate how to recognize improper precharge of gas-padded pulsation dampeners, and even correct while operating. Examples include diagnosis of excess internal leakage, with means to trace further to check valves or other pump internal sources. Fluid property changes, pulsation, and other problems can be diagnosed remotely. Shared is considerable experience gained over the past two years during continuous monitoring on both laboratory and real plant systems. This enables precise knowledge of trends in behavior and root causes so corrective action can be planned, parts and expertise made available, and downtime eliminated or minimized.

INTRODUCTION

Live remote monitoring via the Internet has proven to be a powerful new tool to improve plant productivity and life-cycle cost when used in early failure diagnosis and troubleshooting. In the past, such monitoring and diagnostics work has required bringing nonresident experts with extensive instrumentation to the site after a problem has occurred. This has meant travel costs, operating delays, and the need to reproduce fault conditions once equipment and personnel are in place. Today, the power of the Internet enables the various specialists located globally to see and process live data as effectively as if they were at the site, but without travel and immediately upon capture of events monitored continuously. It also enables trending and recognizing more subtle long-term performance changes not otherwise feasible.

This paper explores a successful global teamwork effort involving high-pressure diaphragm pumps at a plant site in Spain. Dynamic monitoring and pumping system expertise are brought to bear from the plant in Spain, the pump manufacturer in Germany, and from the United States. Recent advances in this area illustrate many new techniques using as examples several high-pressure diaphragm pumps in both laboratory and actual plant applications.

Monitoring of pressure pulsation, check valve opening pressure shock, and other are key elements in condition assessment and diagnostics with positive displacement pumping systems. Numerous real examples illustrate how to recognize improper precharge of gas-padded pulsation dampeners, and even correct while operating. Examples include diagnosis of excess internal leakage, with means to trace further to check valves or other pump internal sources. Fluid property changes, pulsation, and other problems can be diagnosed remotely. Experience gained over the past two years during continuous monitoring on actual systems is shared, which enables trending behavior and root causes. Corrective action can then be planned, parts and expertise made available, and downtime eliminated or minimized.

New, simpler equations are presented to evaluate pump efficiency. Design methods are presented for calculating necessary pump internal and system relief set pressures. Criteria for pressure pulsation and dynamic shock are incorporated. Though simplistic, and not negating the need for rigorous pulsation analysis, the user is provided a reasonable basis upon which to avoid fundamentally incorrect design for pulsation and shock transients.

REMOTE CONDITION MONITORING WITH LIVE DYNAMIC MEASUREMENTS

The essence of live dynamic monitoring via the Internet is shown in the conceptual drawing of Figure 1. As applied to a pumping system in a chemical process plant, shown in this particular case is a high-pressure triplex diaphragm pump. Pressure transducers are shown installed in the hydraulic side of each head, though often many more sensors of various types may also be incorporated. At the heart of the diagnostic measurement system is a network version of monitoring software installed on a local personal computer (PC) server denoted here in "Europe." This PC is equipped with several interface boards to provide signal conditioning and sensing on each channel based on the particular type of sensor: wheatstone bridge, piezoelectric, eddy current, 4 to 20 milliamp, etc. This PC-server also is instructed by one or more "worksheets," running concurrently, to store various data to disk (not shown). Actions or data storage may be continuous, on specific time intervals, and/or based on preset triggers for signal levels or quantities calculated from the signals. Finally, this local server is also equipped with network cards to provide "host" capability for various "clients" accessing the live and stored data from anywhere globally. It is also possible for a client to control the host.

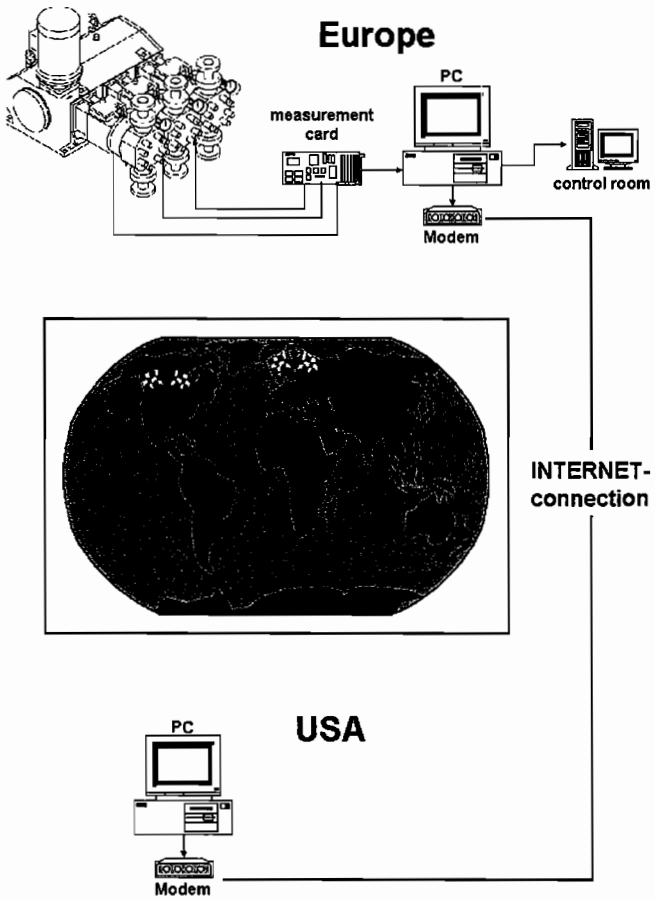

Figure 1. Schematic of the System for Live Remote Dynamic Monitoring for Early Failure Diagnosis and Troubleshooting.

All of this is done with hardware and software currently available from alternative vendor sources, though none will be mentioned or endorsed in this paper. The important thing is to understand the broad capability developed only within the last few years, which is becoming ever more inexpensive and user-friendly.

The next several sections examine the behavior of several diaphragm pump systems through the "eyes" of the monitoring system. Through the course of these discussions, dynamics that are indicative of good health and performance are noted. Likewise, behaviors that indicate problems, or trends that may lead to problems, are also explored. Discussed also are means to determine root cause with advance warning adequate in most cases

to plan for maintenance or correction without disrupting production demands.

BASICS OF DIAPHRAGM PUMPING SYSTEMS AND THE TEST APPARATUS

The primary focus of this paper is the dynamic monitoring system for live remote condition assessment and early failure diagnostics. Before beginning this in earnest, however, it will be necessary to understand a few basics regarding the pumps themselves as well as the particular pumping systems chosen to illustrate the concepts. These systems are both at the operating plant and in the laboratory. Plant experiences illustrate real behavior while the laboratory enables exploring the wide range of fault conditions needed to develop a comprehensive troubleshooting guide.

In all cases, the hydraulically-actuated high-pressure process diaphragm pump is at the heart of the process system. For this reason, a basic understanding of this type of pump is essential, and is therefore provided in the appendix of this paper. A more thorough treatment of these basics is not included here since it has been extensively covered in recent literature to which the interested reader is referred. (Schlücker, et al., 1998; Schlücker, et al., 1997; Vetter, 1994).

The testing results and case histories are organized in the following sections, beginning with laboratory testing in Germany, followed by actual operating data from a chemical process plant in Spain.

LABORATORY TESTING IN GERMANY

Several tests were carried out at the workshop of a pump manufacturer in Germany. The purpose of these tests was to create specific, known fault conditions to see the associated behavior of the pump, particularly with respect to the dynamic pressure graphs of the hydraulic chamber. In this way, when similar behavior of dynamic pressure is seen in actual operating pumping systems, it may be possible to more clearly and definitively conclude the root cause of the problem or condition.

The test system of Figure 2 utilized a triplex polytetrafluoroethylene (PTFE) diaphragm head pump with 52 mm diameter pistons and a 120 mm fixed stroke. The test medium was water. Suction pressure of 5 barg was constant over the complete range of tests. The discharge pressure of 150 barg was created by a manual throttle located downstream of the discharge pulsation dampener based on the pressure gauge on that valve.

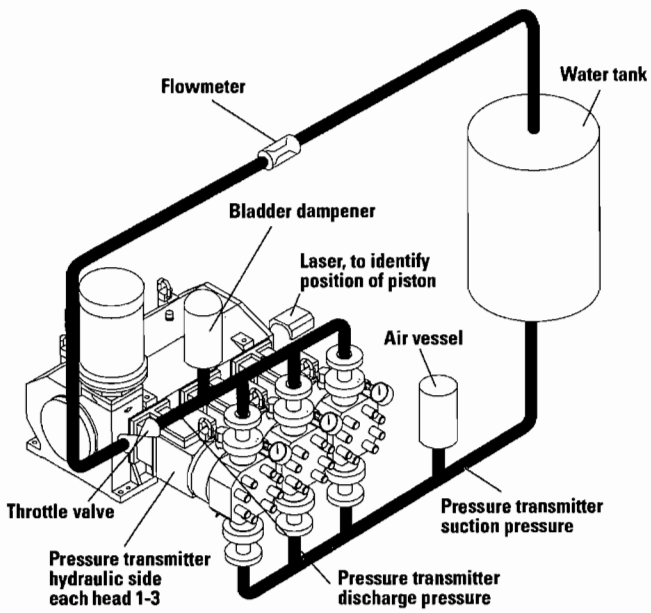

Figure 2. General Arrangement for Dynamic Testing at a Laboratory in Germany.

Suction pipe length was 12,300 mm and discharge pipe length was 13,000 mm with an installed flowmeter. The suction pulsation dampener was a 10 liter air vessel. This was charged online prior to each test with 6 barg air, except as noted, to ensure it to be initially air filled for the test. The discharge pulsation dampener was a single elastomeric bladder-type, nominal volume 4 liters, and precharged to 110 barg. The complete system was instrumented with five pressure transmitters, one in the hydraulic side of each pump head, one upstream of the suction pulsation dampener, and one downstream of the pulsation dampener. The sample rate of the pressure transmitters was 1000 samples per second for all tests. The installation was also instrumented with an optical sensor to detect the piston position. For most of the tests, three speed cases were performed. These were 57 rpm (16 Hz controller setting), 114 rpm (32 Hz), and 178 rpm (50 Hz).

The first test case was with all components in good working order with no fault conditions. This was then followed by several cases with specific fault conditions purposely introduced.

Laboratory Test 30—Pump in Good Working Order

The baseline test was with the pump and all its components in good working order. The process fluid check valves were new, both dampeners in good condition and properly gas charged, and internal valves (replenishment, venting, and pressure limiting) all in like-new condition. The flowrate of the pump at 32 Hz was 4.94 m^3/hr. Venting circulation of hydraulic oil back to the reservoir was approximately 1.8 ml/stroke for heads 1 and 2, and 2.0 ml/stroke for head 3.

For the pump running at 57 rpm (16 Hz controller setting), Figure 3 shows the pressure traces superimposed for the three sensors mounted in the hydraulic side of the heads. For this and many of the following illustrations, the trace for Head 1 is displayed as a solid bold line while the other two are shown in lighter broken lines. This is done solely to make it easier to distinguish the behavior of the single head among the three. Figure 4 shows exactly the same three signals superimposed, but with Head 3 phase-shifted (advanced) 120 degrees and Head 2 advanced 240 degrees. This type of phase-shifted illustration makes it easier to distinguish differences in the behavior of individual heads. Notice in this case, Figure 4 nearly appears to be just one single trace since the three so closely behave the same. While this is true for the pump with all components in good working order, it will be seen that when particular fault conditions exist that affect individual heads uniquely, the differences will appear vividly when phase-shifted and placed on top of one another as in Figure 4.

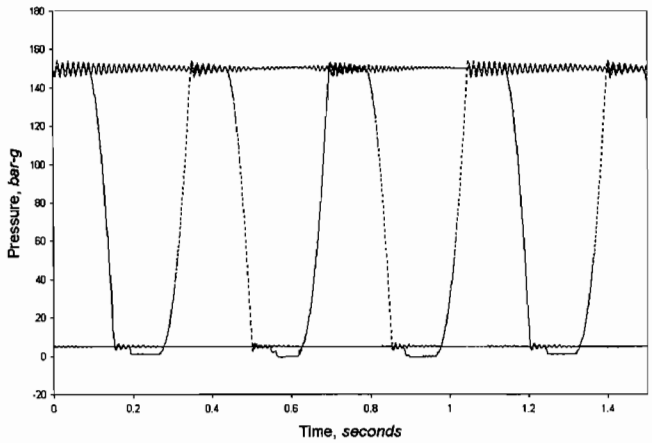

Figure 3. Dynamic Pressure Measurements of Hydraulic Chamber, Three Heads Superimposed, Lab Testing in Germany.

Before proceeding to the various fault conditions, it is worth taking time to explore the general behavior of dynamic pressure on the hydraulic oil side for the healthy pumping system. See also

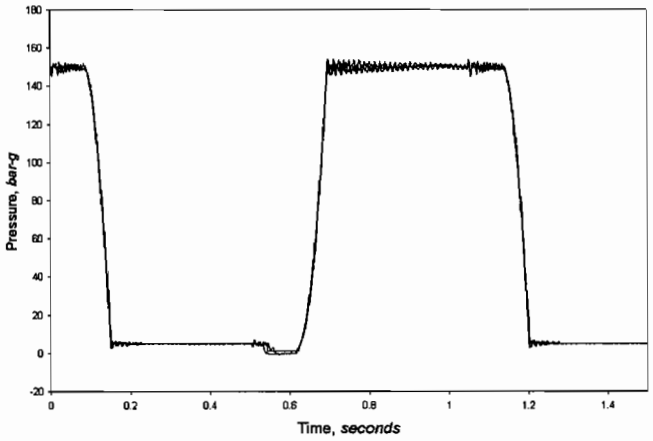

Figure 4. Dynamic Pressure Measurements of Hydraulic Chamber, Three Heads Phase-Shifted and Superimposed, Lab Testing in Germany.

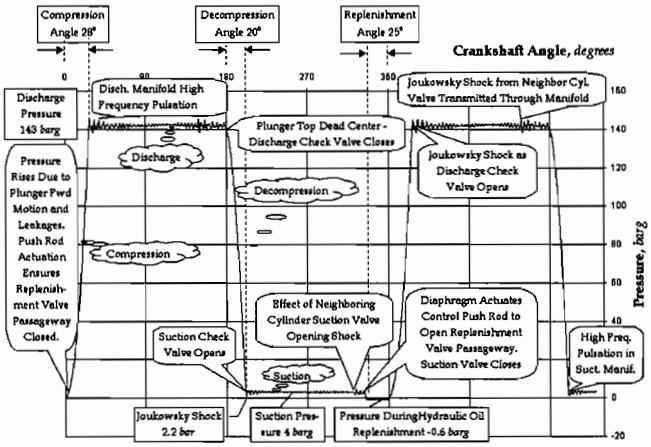

Figure 5. Single Hydraulic Chamber Dynamic Pressure Illustrating Various Behavior and Phenomena.

Figure 5, which pictorially illustrates the following descriptions. Beginning at time zero of Figure 4, the end of the discharge stroke is seen with a cusp or abrupt change in slope as the discharge process check valve closes and decompression begins. The slope becomes steeper across the decompression process because the plunger is accelerating. When the pressure drops to that of mean suction (5 barg), there is a pressure overshoot as the suction process check valve opens, which rings down at high frequency during the initial part of the suction process. The suction process ends with the opening of the hydraulic oil replenishment valve. This is recognized by the pressure drop, which sustains near or slightly below atmospheric. During this *replenishment window*, the oil that leaked out during the preceding cycle is drawn back into the head chamber prior to the next stroke. The width of this *replenishment window* or length of time required to replenish oil therefore is an important indication of the amount of leakage occurring, as will be seen in a later fault condition test. Just prior to the beginning of oil replenishment, note the small dynamic behavior. This is normal and is caused by the transmitted effect through the suction manifold of the opening of the suction process check valve of the neighboring head. At the end of the *replenishment window*, the compression stroke begins. As during decompression, this slope is seen to get steeper across the compression process due to the acceleration of the plunger. Compression ends when the pressure reaches that of mean discharge and the discharge process check valve opens. As with the opening of the suction check valve, this is accompanied by a pressure spike known as the Joukowsky (1898) shock effect, which will be discussed in detail in a later section. Also similar to the suction stroke, this shock dynamic is seen to ring down during discharge and also see the effect of the opening of the neighboring head check valve transmitted, in this case, through the discharge manifold.

Laboratory Test 41—Leaking Discharge Process Check Valve

The effect on the pump of excessive leakage of a discharge check valve was introduced by installing damaged check valve on Head 1 discharge. The flowrate of the pump dropped to 4.3 m^3/hr for the 114 rpm (32 Hz controller setting) speed case versus 4.94 m^3/hr for Test 30 base case. Figure 6 shows the oil-side pressure traces for this speed case superimposed. Again note that the trace for Head 1, with the damaged check valve, is in solid bold while the other two healthy Heads are in broken light lines. Notice that no differences can be detected with this illustration. When the traces are phase-shifted and laid on top of one another, however as before, the differences become very apparent in Figure 7. Here, as in Figure 4 for the base case, the traces for Heads 2 and 3 essentially appear as one (the light broken line). Differences between these are nearly imperceptible. But the trace for Head 1 is markedly different as seen in Figure 7. While compression and decompression begin at nearly the same time as with the healthy heads, the compression is more rapid and steep and the decompression is slower and more gradual. This is because this leaking discharge check valve is providing more backflow and pressurizing the head chamber from the discharge.

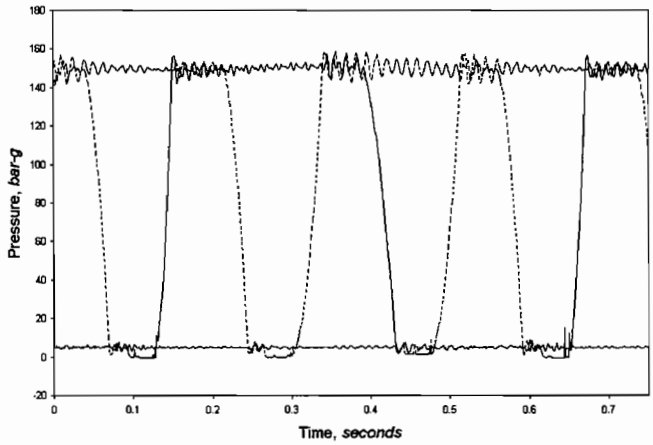

Figure 6. Dynamic Pressure Measurements of Hydraulic Chamber, Three Heads Superimposed, Lab Testing in Germany.

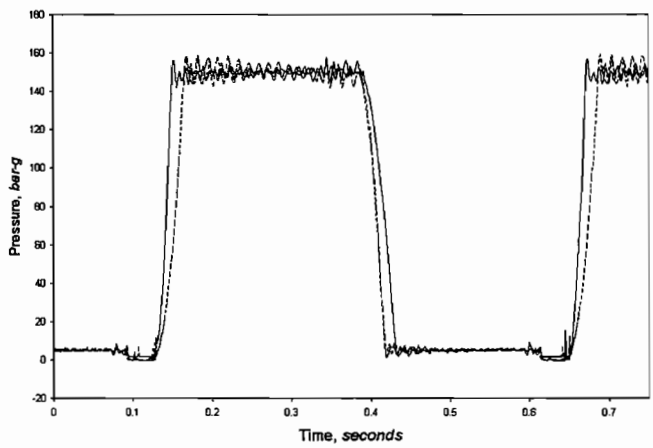

Figure 7. Dynamic Pressure Measurements of Hydraulic Chamber, Three Heads Phase-Shifted and Superimposed, Lab Testing in Germany.

This type of behavior will be seen to be unique to excessive discharge check valve leakage and therefore useful in diagnosing this problem, and specifically which head, when it occurs in a real system.

Laboratory Test 28—Leaking Suction Process Check Valve

In this test, a faulty, leaking suction process check valve was installed on Head 1 suction. All other valves and components were in good working order. This was accomplished by filing an undefined groove in the valve cone. Again for comparison with the prior cases, the flowrate for the 114 rpm (32 Hz controller setting) speed case was 4.13 m^3/hr. This compares with 4.94 m^3/hr for Test 30 base case. The oil-side dynamic pressures for this case are shown in Figure 8 for the phase-shifted superimposed illustration. Here, for the solid bold line for Head 1 with the faulty suction check valve, the compression begins later and takes longer and the decompression begins earlier than for the other two identical good heads. This is because the leaking suction check valve is providing more backflow from the pumping chamber to the suction system, thus reducing the ability of the pump to generate chamber pressure. Notice also that during the discharge process, the pressure has a slight downward tendency toward the end of the process. This is due to the slowing of the piston and the significance of suction valve leakage on the ability of the head to maintain pressure.

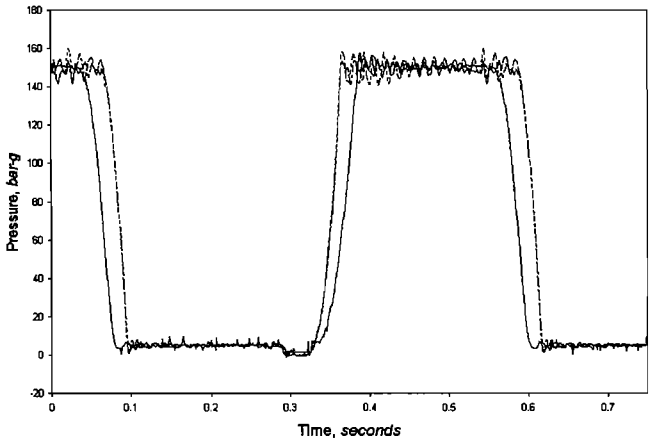

Figure 8. Dynamic Pressure Measurements of Hydraulic Chamber, Three Heads Phase-Shifted and Superimposed, Lab Testing in Germany.

The characteristic type of behavior seen in these traces is seen to be unique to excessive suction check valve leakage and therefore useful in diagnosing this problem, and specifically which head, when it occurs in a real system.

Laboratory Test 25—Leaking Hydraulic Chamber

Leakage of hydraulic oil from the pressurized chamber can occur many ways. All will have essentially the same effect on the pump and its performance, differing only in severity based on the amount of leakage, of course. These pathways include leakage through the:

- Venting valve
- Pressure limiting valve
- Piston rings
- Starting valve
- O-rings
- Replenishment valve

To create excessive hydraulic oil leakage for this test case, the internal pressure limiting valve (PLV) of Head 1 was fitted with a continuous flow venting passage with an oversized groove (refer to APPENDIX A). This resulted in total pump flow measured to be 4.71 m^3/hr. For the 57 rpm (16 Hz controller setting), Figures 9 and 10 show the dynamic pressure traces superimposed and superimposed phase-shifted, respectively. Figure 10 shows a small delay in the compression and a small advance in the decompression, but these differences are indeed rather slight in appearance considering the severity of the leakage, and may not be very perceptible in a real system. What is very evident, however, and obvious for both illustrations, is the significant increase in the length of time the replenishment valve is open for Head 1 versus the other heads.

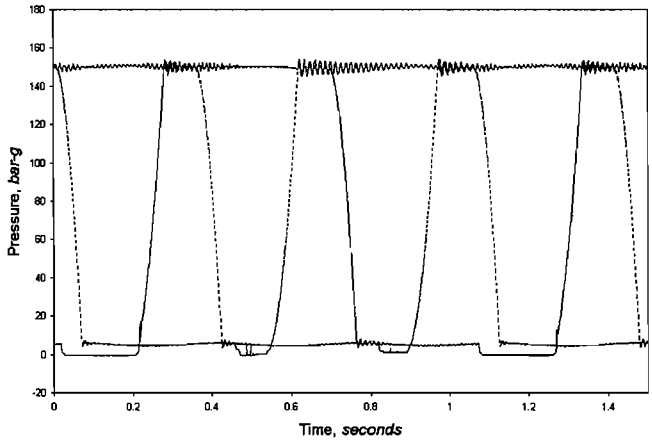

Figure 9. Dynamic Pressure Measurements of Hydraulic Chamber, Three Heads Superimposed, Lab Testing in Germany.

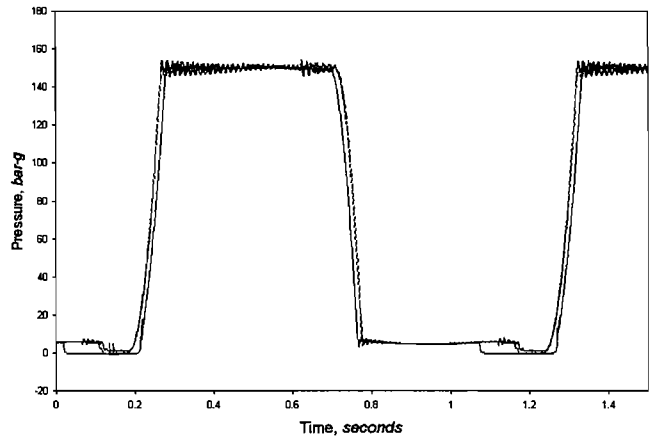

Figure 10. Dynamic Pressure Measurements of Hydraulic Chamber, Three Heads Phase-Shifted and Superimposed, Lab Testing in Germany.

It has been learned that a large replenishment time is uniquely indicative of excessive hydraulic oil leakage from the pressurized chamber. What is not clear or discernable, however, is which of the six leakage paths listed above is or are responsible for such an excessive leakage, should it be detected in actual operation for any particular head.

Laboratory Test 24—Overcharged Discharge Pulsation Dampener

To simulate the effect of improper charge on a pulsation dampener, the gas bladder type unit on discharge was charged up to 170 barg. Hence, no dampening would exist whatsoever. For the 114 rpm (32 Hz) speed case, the pressure traces are shown in Figure 11. Notice the very significant low frequency dynamic component apparent during the discharge stroke. There are in fact six "humps," three small and three large, within each full crank

revolution. These humps can be seen to coincide with the flow-forcing behavior often described in the literature for the triplex pump (Figure 12). Notice the shapes of the flow forcing with six peaks per crank revolution, for triplex (i = 3) and for volumetric efficiency between 0.9 and 1.0.

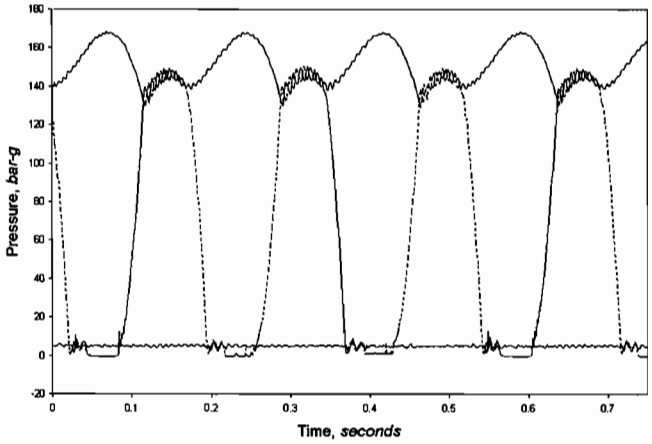

Figure 11. Dynamic Pressure Measurements of Hydraulic Chamber, Three Heads Superimposed, Lab Testing.

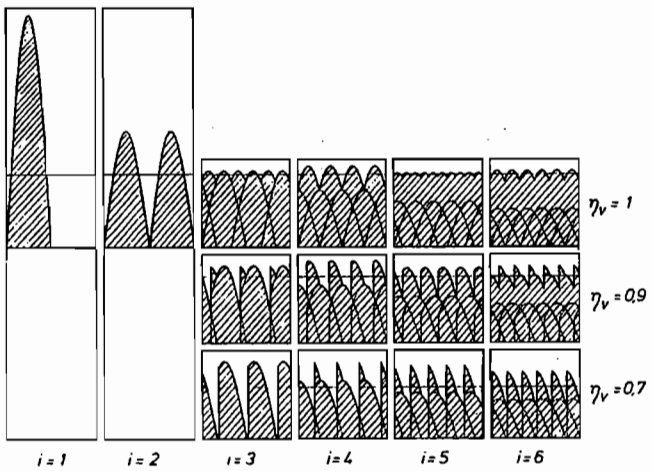

Figure 12. Flow Forcing Characteristics for Various Numbers of Pump Heads and Volumetric Efficiencies. (Courtesy Turbomachinery Laboratory (Schlücker, et al., 1999))

This test system for this fault condition case is unique however, in that the effective discharge system is very stiff (very little compressibility) due to the fact that the discharge throttling valve is relatively close to the pump. Hence, it is important to note that this observed behavior of dominant six-times-running-speed component of pulsation does not necessarily equate to an improperly charged pulsation dampener. It is possible to have improper charge without predominant 6×, and vice versa. This behavior and any resulting relationship are very much a function of the acoustic frequency response characteristics of the attached piping system. This issue is addressed further in a later section of this paper.

CONTINUOUS ONLINE MONITORING AT THE OPERATING PLANT IN SPAIN

At a chemical manufacturing plant in Spain, several pumps and other types of process equipment have been instrumented for 24-hour continuous monitoring. For over two years now, scores of pressure, strain, and other signals are captured at rates up to several thousand samples per second. As described above, these live and historical data are available via the Internet equally readily to globally remote client PCs as they are at the plant site itself. This enables, at any time without travel costs or delays, technical specialist assistance from in-house, equipment manufacturers, consulting firms, or others at the discretion of the operating plant.

A pump of the same frame size but with larger heads than that used in the laboratory tests is among the equipment monitored at the plant in Spain. Described here are the events that unfolded following the appearance of an irregular or corrugated shape in the cylinder dynamic pressure trace during the suction stroke (compare Figure 13 and Figure 3). The problem would be diagnosed as overcharge of nitrogen in the suction pulsation dampener and resolved online without shutting down.

Case History

This pump is equipped with dual-chamber pulsation dampeners on both suction and discharge. This type of dampener utilizes an intermediate fluid, usually hydraulic oil, between a nitrogen-filled bladder in the upper chamber and a diaphragm that faces the process in the lower chamber.

During a shutdown, one of the maintenance procedures was to reset the gas precharge in the dampeners. Upon restart, the cylinder head pressure traces appeared as seen in Figure 13. In this and the following several figures, one pressure trace of the three superimposed is in bold for clarity. Notice the very rough appearance of pressure during the suction stroke, shown also in the zoom detail in Figure 14. The trace in bold exhibits a sustained drop in pressure from time A to time B and again from time C to time D. The mean pressure during both these time periods should instead be nominally equal to the mean suction pressure, about 58 psig in this case. The candidate explanations for this initially included the following:

- Excessive amount of nitrogen precharge in the bladder of the upper chamber of the damper,
- Cavitation occurring on pump suction, or
- Insufficient oil in the intermediate chamber of the dampener between the nitrogen-filled bladder and the diaphragm facing the process.

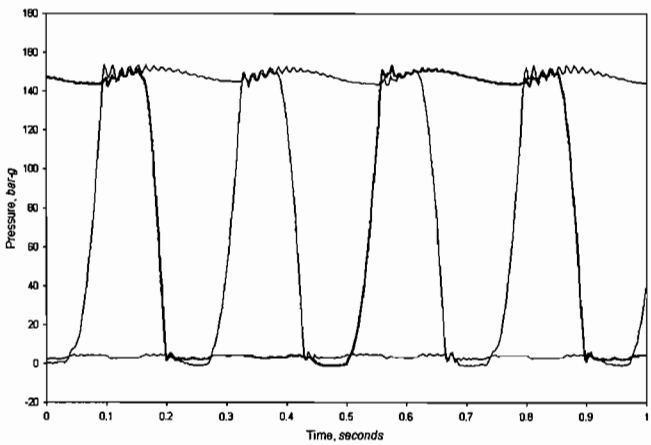

Figure 13. Dynamic Pressure of Hydraulic Chamber, Three Heads Superimposed, Operating Plant in Spain.

Cavitation was believed to be an unlikely cause since the mean suction pressure of 58 psig is evident during other segments of time during the suction stroke. This is well above the net positive suction head required ($NPSH_R$) for the pump even for much higher operating speeds. Likewise, it was concluded that insufficient intermediate fluid could not explain this behavior. Hence, the possibility of excessive gas precharge remained the only identified candidate cause.

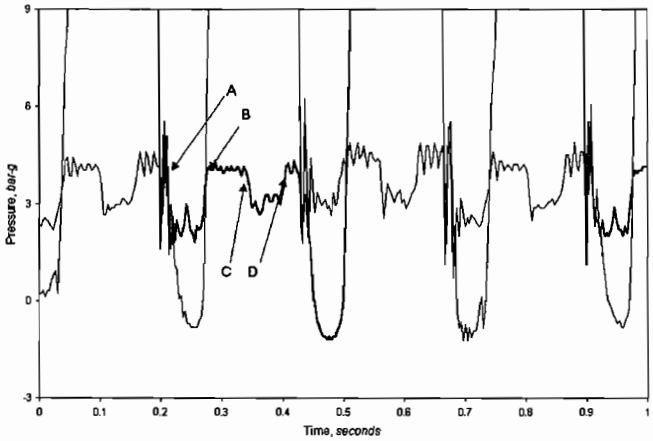

Figure 14. Dynamic Pressure of Hydraulic Chamber, Three Heads Zoom on Suction, Spain.

It was decided to bleed a small amount of gas off the suction dampener while monitoring the dynamic pressure traces. This was done with a mechanic in the field communicating by hand-held radio with an engineer in a nearby office building who, in turn, was on the phone with an engineer in Houston monitoring the live dynamic pressure traces. This was done in a slow deliberate process that first produced the change in the dynamic pressures as shown in Figure 15 and, zooming in on suction, Figure 16. Notice that the pressure dip that existed during the time duration from C to D in Figure 14 has disappeared in favor of the normal expected mean suction pressure. This suggests that the scenario of excessive precharge may have been correct and bleeding some pressure off is the correct thing to do. Notice that the pressure dip in the bold curve sustained below the mean suction pressure in the interval from time A to time B still exists, however. It was decided to bleed an additional small amount of nitrogen off the suction dampener. Doing so produced the pressure traces shown in Figure 17 and, zooming on suction, Figure 18. Notice this is a very healthy looking pressure profile across the entire suction stroke and the immediate problem has been solved.

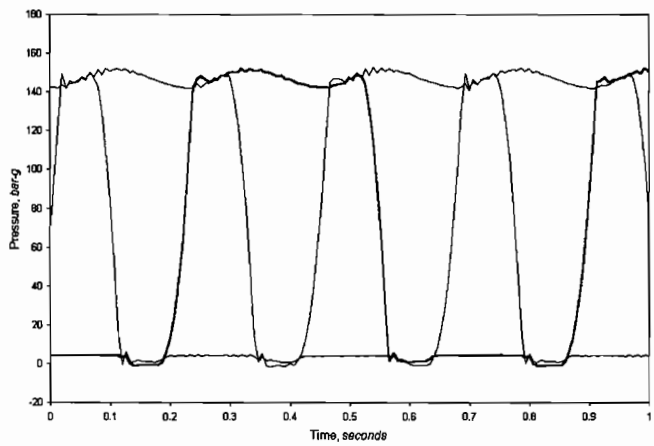

Figure 15. Dynamic Pressure of Hydraulic Chamber, Three Heads Superimposed, Suction Dampener Overcharge Partially Resolved, Spain.

It should be noted that while the above procedure resulted in achieving a nitrogen charge and dampener effectiveness at an acceptable functioning level, it is not necessarily ideal. The charge could still be other than optimal and at another speed, for example, the symptom of the problem could recur. It was decided that a plan should be developed to enable correct charging online without shutting down. The procedure that was developed and will be tested and implemented in the future is described in the Appendix of this paper.

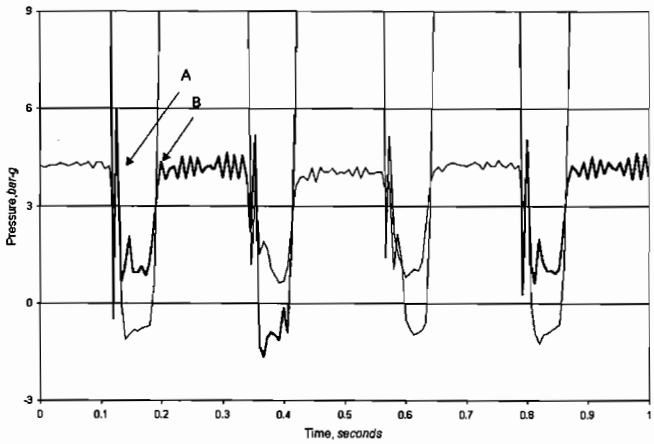

Figure 16. Dynamic Pressure of Hydraulic Chamber, Three Heads Zoom on Suction, Suction Dampener Overcharge Partially Resolved, Spain.

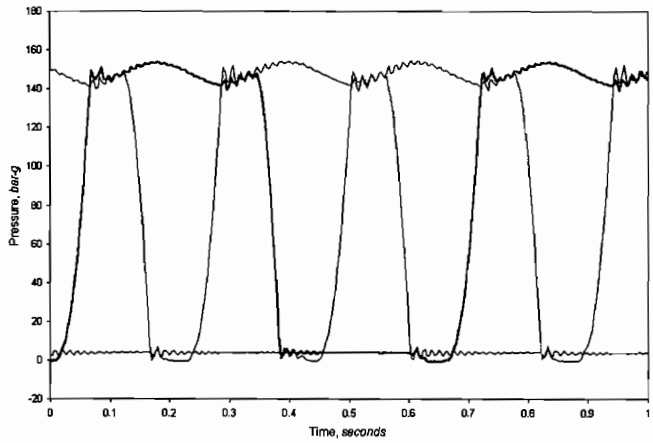

Figure 17. Dynamic Pressure of Hydraulic Chamber, Three Heads Superimposed, Suction Dampener Overcharge Fully Resolved, Spain.

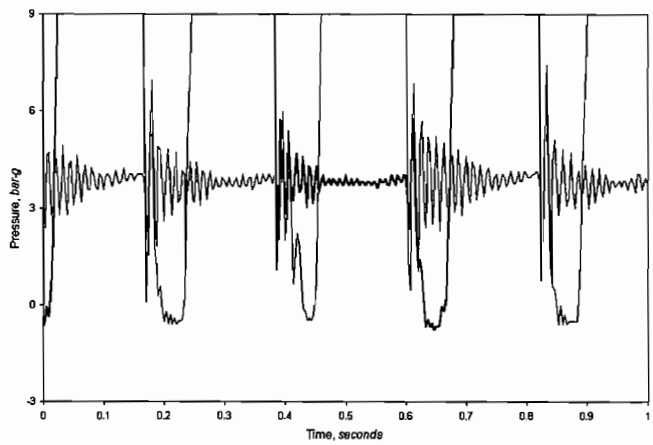

Figure 18. Dynamic Pressure of Hydraulic Chamber, Three Heads Zoom on Suction, Suction Dampener Overcharge Fully Resolved, Spain.

MEAN AND DYNAMIC PRESSURE ISSUES IN DESIGN

Presented here are the equations and relationships between and among the many pressures important in design and specification of the pump, piping, and other components comprising the *pumping system.* These include normal operating, maximum

operating, design operating, pump internal relief setting, process system relief setting, tolerances in setting pump internal relief and system relief settings, Joukowsky shock pressure spike, and piping pulsation magnitudes. An example will be given. Issues such as vapor pressure, acceleration head, and NPSH are covered extensively in the literature and are outside the scope of treatment here.

First, the well-known slider crank equations for plunger position and velocity are presented.

$$x(t) = r[1-\cos(\omega t)] - l + \sqrt{l^2 - r^2\sin^2(\omega t)} \tag{1}$$

$$\dot{x}(t) = r\omega\sin(\omega t)\left[1 - \frac{r\cos(\omega t)}{\sqrt{l^2 - r^2\sin^2(\omega t)}}\right] \tag{2}$$

Joukowsky, in a landmark paper (1898), developed the mathematical treatment for classical waterhammer addressing the sudden pressure shock wave front caused by a rapidly actuating valve. For the internal check valves of the pump, this Joukowsky Shock effect is presented here in the form:

$$\Delta P_J = 10^{-2}\rho(a)\Delta V \tag{3}$$

where, at the time, t, of valve opening, the velocity jump in the piping, ΔV, is:

$$\Delta V = 10^{-3}\dot{x}(t)\left(\frac{\phi}{d}\right)^2 \tag{4}$$

Hence, this pressure shock effect is:

$$\Delta P_J = 10^{-5}\rho(a)\dot{x}(t)\left(\frac{\phi}{d}\right)^2 \tag{5}$$

At this point, it is possible to develop the relationships necessary to establish the various design, operating, and relief pressures related to the pump and piping. Of particular criticality are establishing the relief set pressures for the pump internal pressure limiting valves (PLVs), P_{PRV}, and for the discharge piping, P_{RD}. Also important to recognize are the uncertainty or variability associated with the setting of these relief pressures, δP_{PRV} and δP_{RD}, respectively. Therefore, the minimum values for these relief pressures in design of the system must not be less than the following:

$$P_{PRV} \geq P_e + \Delta P_J + \delta P_{PRV} \tag{6}$$

$$P_{RD} \geq P_{PRV} + \delta P_{PRV} + \delta P_{RD} + P_{RM} \tag{7}$$

where P_{RM} is the required margin between the minimum relief pressure of the piping system and maximum relief pressure of the pump internal PLVs.

• *Example 1*—The relief set pressures for the pump internal PLVs and discharge piping system are to be determined for a pumping system utilizing a diaphragm pump with the following data obtained from the basic data sheet.

$S = 120$ mm
$l = 450$ mm
$P_e = 152$ barg
$\phi = 65$ mm
$N_R = 182$ rpm
$P_i = 4$ barg
$d = 50$ mm
$\rho = 1.162$ kg/l

The following additional data are provided by the project team and pump manufacturer.

$\varepsilon f = 3.17$
$K_h = 73\times10^{-6}$ bar^{-1}
$P_{RM} = 2$ bar
$\varepsilon_h = 1.89$
$\delta P_{PRV} = \pm 5$ bar
$\eta_{Gp} = 0.5\%$
$Kf = 44.5\times10^{-6}$ bar^{-1}
$\delta P_{RD} = \pm 0.5$ bar
$\eta_{Gh} = 1.5\%$

• *Solution*—Utilizing the equations developed and presented above, the following can be determined.

$$\Delta P = P_e - P_i = 148 \text{ bar}$$
$$\eta_V = 1-\eta_K-\eta_G = 1-4.157\%-2.72\% = 93.4\%$$
$$a = \sqrt{\frac{100}{K_f\rho}} = 1391 \text{ m/s}$$
$$x(t_2) = \eta_K S = 5 \text{ mm}$$
$$t_2 = 0.23086 \text{ s} \tag{8}$$
$$\dot{x}(t_2) = 428.2 \text{ mm/s}$$
$$\Delta P_J = 10^{-5}\rho(a)\dot{x}(t_2)\left(\frac{\phi}{d}\right)^2 = 11.7 \text{ bar}$$
$$P_{PRV} \geq P_e + \Delta P_J + \delta P_{PRV} = 168.7 \text{ barg}$$
$$P_{RD} \geq P_{PRV} + \delta P_{PRV} + \delta P_{RD} + P_{RM} = 176.7 \text{ barg}$$

Therefore, this piping system should be rated to at least 177 barg on discharge and the internal relief setting of the pump should be set to 169 barg.

CONCLUSION

The use of live continuous monitoring of dynamic pressure in critical process equipment has been found to be an invaluable tool in condition assessment, in early diagnosis of trends indicating a failure or other problem development, and in correcting some problem online even without shutting down. Essentially all the additional learnings and conclusions made here are either a direct or indirect result of the recent development, power, affordability, and user-friendliness of these hardware and software systems.

With respect to high-pressure hydraulically-actuated process diaphragm pumps, many *signatures* of dynamic behavior have been identified that indicate existence of specific fault conditions and root causes. This advance knowledge of behavior, trends, and problems enables earlier problem resolution and the ability to plan for time and resources to be applied during regularly schedule maintenance. Specifically:

• *Discharge product check valve excessive leakage* is indicated on a head when, versus the other cylinders, early and more rapid pressurization occurs during compression, depressurization is delayed and slower, while oil replenishment time still looks normal (Figure 7),

• *Suction product check valve excessive leakage* is indicated on a head when, versus the other cylinders, later and slower pressurization occurs during compression, depressurization is early, while oil replenishment time still looks normal (Figure 8),

• *Excessive hydraulic chamber leakage* is indicated on a head when the oil replenishment time at the end of the suction stroke is very long (Figures 9 and 10),

• *Gas-pad type pulsation dampener has lost effectiveness* through either over- or under-charge of gas is indicated when relatively higher magnitudes of low frequency dynamics occur. Common frequencies are 1, 2, 3, and 4 times the base pulsation frequency, which is the number of heads times running speed (Figure 11),

• *Gas-pad type suction pulsation dampener is overcharged with gas* when the pressure traces during suction experience sustained pressure dips below mean suction pressure for periods near relative high suction flow demand (Figures 14 and 16). This would be subsequent to suction product check valve opening and again in the

middle of the suction stroke, not to be confused with the oil replenishment window at the end of suction. A metallic impacting noise may also be audible from the dampener.

There are two methods that show promise to be able to reestablish proper gas charge on a gas-pad type pulsation dampener online without shutting down. One is to overcharge the gas pressure above the mean operating pressure and then very slowly bleed off gas while viewing the dynamic pressure traces. When low frequency dynamic pressure magnitudes return to normal levels, a reasonable, though not necessarily ideal, gas charge has been achieved. The second method is proposed as part of this work that utilizes calculations and a *receiver vessel* sized specifically for the application to reestablish the correct vendor-recommended gas charge.

Simple equations are developed in the Appendix that enable easy calculation of expected performance from the hydraulically actuated diaphragm pump, which work also for the simple plunger pump.

Simple equations are presented to enable setting the operating, relief, and design pressures for a pumping system incorporating adequate margins for pressure dynamics and variability in set pressures. This includes easy calculation of the Joukowsky dynamic pressure shock effect. Together, this gives the user the ability to avoid the common problem of developing a system that provides inadequate pressure margins that can lead to premature relief events involving rupture disks, relief valves, and pump internal pressure limiting valves.

A simple method is proposed in the Appendix to enable estimating the acoustic natural frequencies of pressure pulsation in a pump and piping system, at least for relatively simple systems without a lot of pipe branches. These frequency estimates are compared with pump fundamental excitation frequencies to enable recognizing if a problem may be expected at one or more pump speeds, which would indicate a more detailed pulsation study to be warranted. Simple estimating methods are also presented to help the user understand where, physically, in a piping system the peak levels of pulsation may be expected that may warrant particular attention to piping support in those areas.

Finally, a review of the workings of the hydraulically actuated diaphragm pump concisely summarizes a considerable amount of existing literature. This also discusses important fundamental issues with product check valves, whose optimal design is so often critical to high reliability and low life-cycle cost of the equipment.

NOMENCLATURE

a	(m/s)	Acoustic wave velocity
d	(mm)	Connected pipe diameter for Joukowsky shock calculation
C_b	(-)	Boundary condition of piping termination remote from pump
f_{ni}	(Hz)	i^{th} pipe mode acoustic natural frequency, $I = 1, 2, 3, \ldots$
K_f	(1/bar)	Process fluid compressibility
K_h	(1/bar)	Hydraulic oil compressibility
ll	(mm)	Connecting rod length
L	(m)	Overall piping system length from a pump to a boundary
m_i	(kg)	Mass of process fluid evolved per head per stroke
N	(rev/min)	Pump speed
N_R	(rev/min)	Rated pump speed
P_e	(barg)	Pump outlet (discharge) pressure
P_i	(barg)	Pump inlet (suction) pressure
P_{PRV}	(barg)	Set pressure of the pump internal pressure limiting valve (PLV)
P_{RD}	(barg)	Relief device set pressure in the pump discharge system
P_{RM}	(barg)	Margin of discharge system relief above pump internal relief
r	(mm)	Crank radius (half of plunger stroke)
S	(mm)	Plunger stroke
t	(s)	Time
t_1	(s)	Time of plunger zero velocity at end of suction (BDC)
t_2	(s)	Time of discharge check valve opening
t_3	(s)	Time of discharge check valve closing
t_4	(s)	Time of plunger zero velocity at end of discharge (TDC)
t_5	(s)	Time of suction check valve opening
t_6	(s)	Time of snifter valve opening
t_7	(s)	Time of snifter valve closing
$\forall_c$	(mm^3)	Process fluid volume in chamber at the end of suction stroke
$\forall_{hd}$	(mm^3)	Hydraulic oil dead volume
$\forall_{hi}$	(mm^3)	Hydraulic oil volume, end of suction stroke
$\forall_{he}$	(mm^3)	Hydraulic oil volume, end of discharge stroke
$\forall_{sw}$	(mm^3)	Plunger swept volume
V_{fd}	(mm^3)	Process fluid actual dead volume in the chamber
$\forall_{fdo}$	(mm^3)	Process fluid ideal dead volume
v_{fe}	(mm^3/kg)	Specific volume of process fluid at pump exit
v_{fi}	(mm^3/kg)	Specific volume of process fluid at pump inlet
v_{he}	(mm^3/kg)	Specific volume of hydraulic oil at pump exit
v_{hi}	(mm^3/kg)	Specific volume of hydraulic oil at pump inlet
x(t)	(mm)	Plunger position at time, *t*
$\dot{x}(t)$	(mm/s)	Plunger velocity at time, *t*
ΔP	(bar)	Pressure developed across the pump
ΔP_J	(bar)	Joukowsky pressure surge
ΔV	(m/s)	Velocity jump in piping at instant pump check valve opens
ε_f	(-)	Process fluid ideal dead volume ratio
ε_h	(-)	Hydraulic oil dead volume ratio
ρ	(kg/l)	Process liquid density
η_G	(-)	Head efficiency effects factor for volumetric efficiency
η_{Gh}	(-)	Pump internal leakage effect factor per 100 bar at ΔP at N_R
η_{Gp}	(-)	Product check valve leakage effects factor at rated pump speed
η_K	(-)	Compressibility effects factor for volumetric efficiency
η_V	(-)	Volumetric efficiency of the pump
ϕ	(mm)	Plunger bore
ω	(1/s)	Circular frequency of pump speed

APPENDIX A

BASIC OPERATION OF THE HYDRAULICALLY ACTUATED PROCESS DIAPHRAGM PUMP

The hydraulically-actuated high-pressure diaphragm pump uses a crankshaft driven plunger to pressurize a hydraulic oil reservoir and diaphragm to act upon the process fluid (Figure A-1). Since only hydraulic oil comes in contact with the mechanical shaft and seals of the pump, it is sealed and leak-free on the process side. This type of pump is suited to relative high pressure, low flow, and/or to metering applications handling fluids that are toxic, environmentally sensitive, corrosive, abrasive, poor lubricity, or sterile.

The hydraulically-actuated diaphragm pump internals incorporate several additional ancillary functions.

- Maintain constant volume of the hydraulic fluid by automatic leakage replenishment
- Provide internal pressure limiting to avoid overloading on the hydraulic side
- Vent air bubbles present in the hydraulic fluid

Figure A-1 shows the important assemblies of a hydraulically actuated diaphragm pumphead.

- Venting valve (VV)

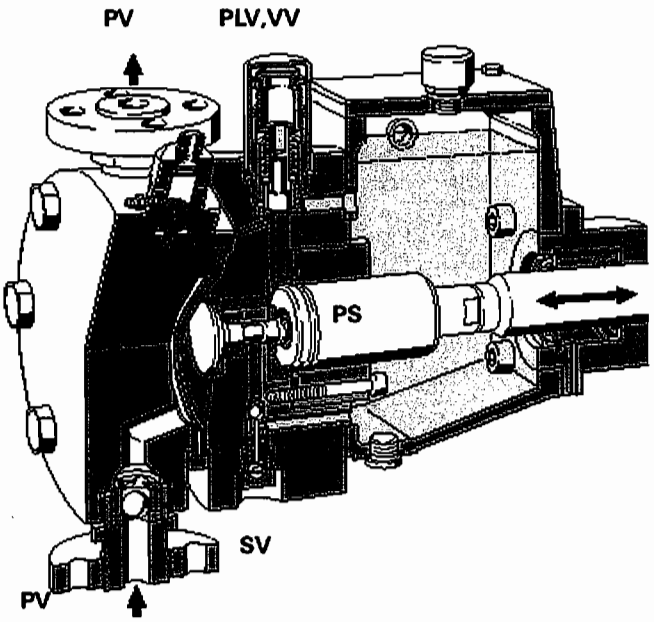

Figure A-1. Cutaway of the PTFE Diaphragm Pump Head of Triplex Pump Used in Lab Tests.

- Oil replenishment (snifting) valve (SV)
- Pressure limiting valve (PLV)
- Product check valves (PV)

Venting Valve

Air bubbles that result from a variety of effects can reduce flow performance and accuracy and so must be vented. Two alternative vent valve designs are *volumetric* and *continuous*.

The *volumetric* vent valve evolves from the pumping chamber a precisely defined fixed volume of hydraulic oil and any air bubbles contained (Figure A-2). This occurs at the start of each discharge stroke when the shouldered plunger is forced upward. During the suction stroke, a spring returns this plunger to its starting position. This displaced volume is independent of speed, stroke length, viscosity, and discharge pressure.

The *continuous flow* vent valve is somewhat similar in that it has a spring-loaded shouldered plunger and is part of the *combination valve*, which includes the pressure limiting function described below. However, it is open virtually all the time (save the replenishment window). With the continuous flow vent valve, volume per stroke does vary as a function of speed, viscosity, and pressure.

The return of air is prevented by an integrated nonreturn valve for both valve types. The volume vented, by design, varies from 0.2 to 1.5 percent of the swept volume. Larger pumps use smaller venting percentages.

Oil Replenishment (Snifting) Valve and Control Push Rod

Hydraulic oil leakage through the vent valve and other pathways is automatically replenished at the end of the suction stroke. When the diaphragm reaches the back of the chamber, it actuates the *control push rod*, which opens the connection to the snifting valve (SV) while providing a smooth contour against which the diaphragm rests (Figure A-3). Any remaining excursion of the plunger is accommodated by oil drawn through this valve into the chamber. These valves are typically light preset ball type, as shown in Figure A-4, without springs and open with minimal vacuum.

Pressure Limiting Valves

Pressure limiting valves (PLV) of the types shown in Figure A-5 protect the pump head and drive element against overload in case of deadheading or other source of excessive back pressure. They

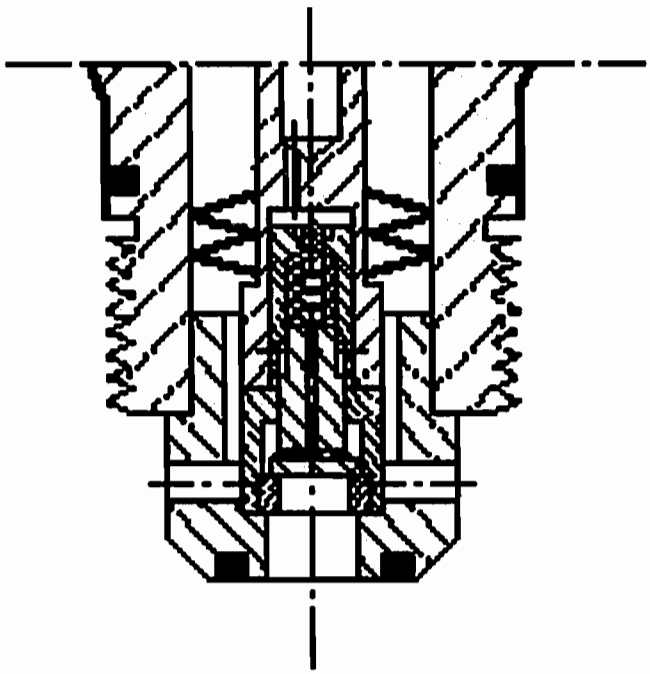

Figure A-2. The Volumetric Vent Valve.

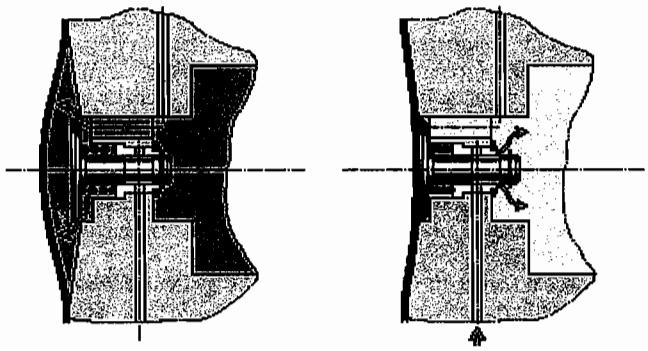

Figure A-3. The Control Push Rod.

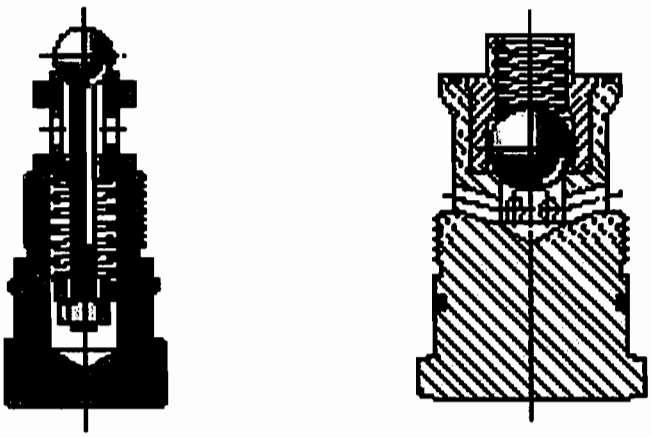

Figure A-4. Hydraulic Oil Replenishment (Snifting) Valves.

are typically full stroke valves and open completely when the set pressure is exceeded, even for short-term overpressure. The hydraulic oil is vented to the reservoir.

Plunger Seal

Action of the plunger and seals in hydraulic oil rather than the process constitutes a distinct advantage of the diaphragm pump

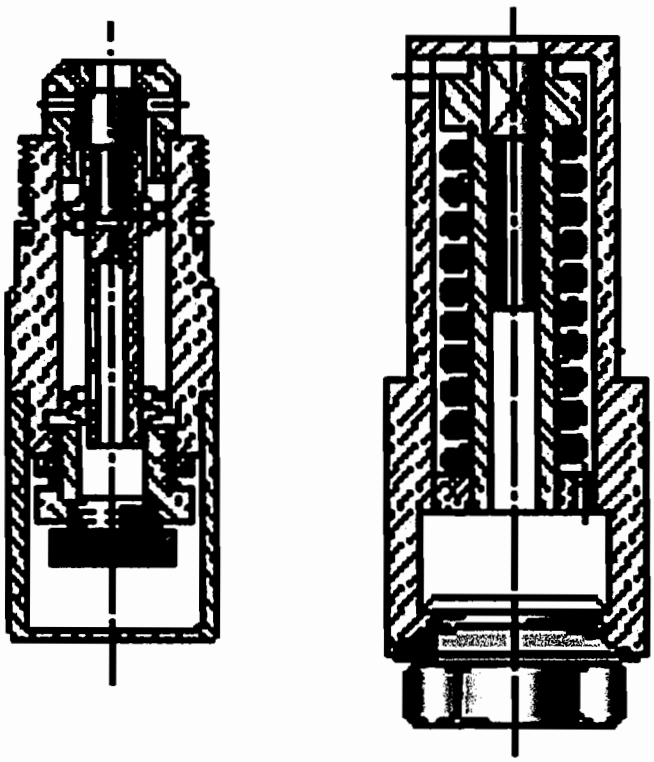

Figure A-5. Pressure Limiting Valves.

over the conventional plunger pump (Figure A-6). Still, the plunger seal (ps) is critical to uptime and life-cycle costs. For reduced maintenance and higher reliability and efficiency, packing and chevron rings are avoided in favor of two proven plunger sealing designs: piston rings and ground-in seals. Piston rings are practically used up to about 350 barg. The ground-in seal is preferred for diameters less than 20 mm, based on reliability and economics, and also for pressures greater than 350 barg for strength reasons.

Product Valves

About 90 to 95 percent of all product valve (PV) designs are satisfied successfully with conical or crowned sealing geometries (Figure A-7). Though, taken by itself, this statement can be misleading due to the many important detailed factors involved. Optimal design of the product valves is extremely challenging due to the need to consider many widely varying parameters. These include ranges of flowrates, process corrosivity, temperature, viscosity, etc. Opposite this, there are criteria to be met such as metering accuracy, efficiency, mean time between failure, maintenance and other costs, noise and vibration, and others. Good design depends on applying the best technology in mechanical engineering, fluid mechanics, finite element analysis, and materials engineering so the valves are highly functional, smooth and quiet, and have long life. Specifically, across the entire range of operating conditions, the valves must possess:

- Soft function
- Low closing energy
- Tightness
- Wear resistance
- Low pressure loss
- Resistance to corrosion

The closing action of the check valve may be divided into three stages, as shown in Figure A-8

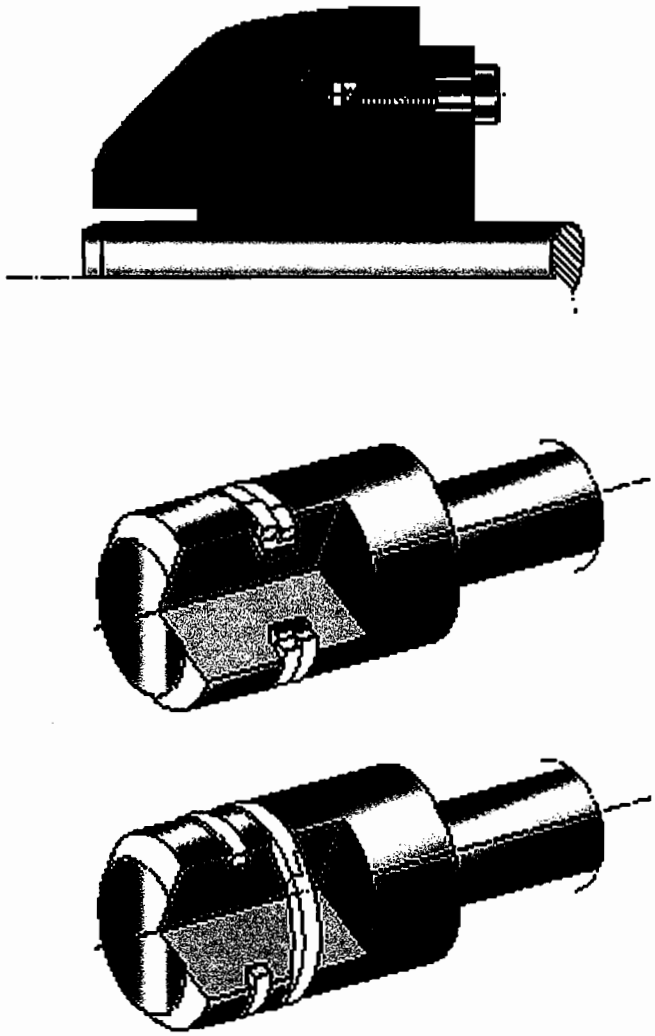

Figure A-6. Plunger Seal Types, Ground-In Seals and Piston Rings.

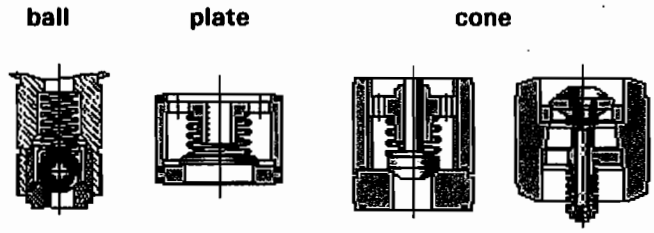

Figure A-7. Various Types of Product Check Valves.

- *Acceleration*—The closing body is leaving the upper dead point induced by force of pressure differential, spring force, and gravity
- *Damping*—The valve body decelerates due to fluid shear forces
- *Impact*—The closing body experiences impulse abruptly bringing its velocity to zero through impact of the sealing surfaces. Both elastic and inelastic deformations occur that cause wear and pitting, respectively.

This total strain energy with energy in Stage III is equal to the kinetic energy at the end of Stage II, according to $E = \frac{1}{2} mv^2$. The larger this value, the larger is the wear and pitting of the valve and seat. Therefore, an important effect of damping is to reduce this wear and pitting. Sources of damping during Stage II include:

- Process fluid viscosity and entrained/imbedded particles, both in the flow passageways and in the stem guide

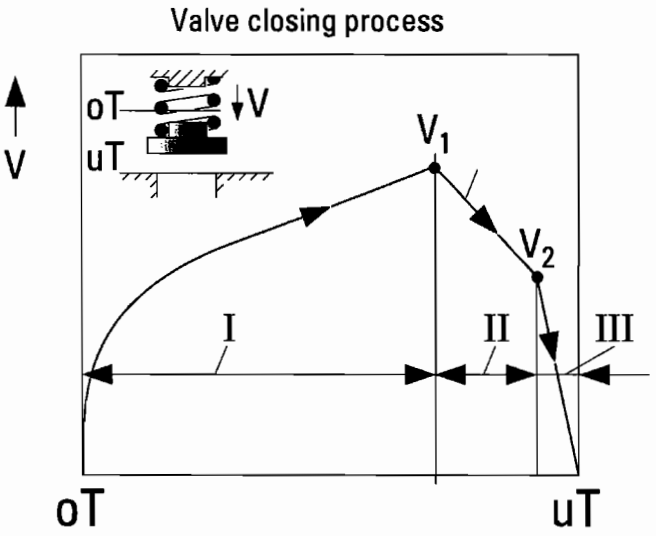

Figure A-8. Velocity Versus Time Plot of Three Stages During Closure of the Product Check Valve.

- Elastomeric auxiliary sealing
- Elastic or mass improved valve parts

The first is inherent to the fluid, but its effect can be influenced by the plug profile and in the design of the stem and guide. Limited success has been achieved with elastomeric sealings primarily due to limited chemical stability. The elastic and mass improved valve bodies (combined with optimal springs) generally offer the best opportunity to design in effective damping.

Material selection plays a key role in valve wear but hardness is not the only important property. Consider that, in Stage III, the compressive energy is the same for the valve closing body (SK) and the valve seat (S). The triangle diagram of Figure A-9 depicts the local elastic deformation characteristics.

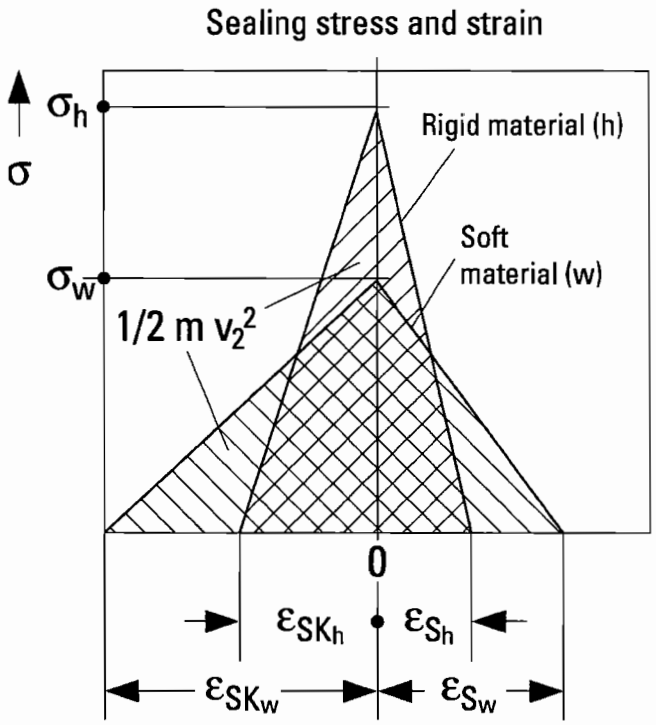

Figure A-9. Stress-Strain Relationship for Product Check Valve Sealing Surfaces in Closing Stage III (Impact).

The kinetic energy at the beginning of the impact phase has to be fully absorbed by the material and therefore corresponds to the hatched area. The size of deformation results in a typical compression σ. Since a more rigid material (h) tends to have a higher elastic modulus, the sum of εsk and εs is smaller, but at equal springs and masses the energy input (area of the triangle) remains unchanged. That means that more rigid materials generally create higher compression in the sealing area. The correlation is approximately linear. Twice the elastic modulus produces approximately twice the compressive stress. Therefore, the use of a more rigid material is more expensive and makes sense only if the ratio of σ *admissible* to σ is increasing. Experiences with methanol confirm this. Tungsten carbide valve parts have shown wear of the valves (outbreaks) after a short running period. In this case, with valve parts made of high-strength steel, however, satisfactory running periods and low life-cycle costs were accomplished. These statements are only valid as long as there are no abrasive particles in the fluid. If abrasive particles are jammed into the sealing area, the only predominant factors are the differences in hardness between the sealing area and the particles. The best economical solution therefore is to use expensive hard and most rigid materials. Experiences with silicates and Raney-Nickel confirm this. Finally, by installing valve parts of silicon-nitride or tungsten carbide, it was possible to achieve quite acceptable life-cycle costs.

POSITIVE DISPLACEMENT PUMP EFFICIENCY AND PERFORMANCE

Equations are presented in this section for calculating volumetric efficiency and flow performance consistent with common industry terminology. These are developed for the hydraulic diaphragm pump, but are valid for a standard plunger pump when either the volume or the compressibility of the hydraulic oil is set to zero.

The overall volumetric efficiency of the pump, η_V, is given by,

$$\eta_V = 1-\eta_K-\eta_G \qquad \text{(A-1)}$$

In a healthy pump, the predominant effect on efficiency is the fluid compressibility effects factor, η_K. It can be as little as a few percent but often as much as 20 to 30 percent or more. The head efficiency effect factor, η_G, which includes leakage of the process and hydraulic fluids and pump head flexing, is usually in the range of one to three percent. Values of η_G greater than five percent generally are indicative of severe leakage problems.

Evaluation of the compressibility effects factor, η_K, begins with some definitions and fundamental physical relationships involving the pump and fluid basic data (Figure A-10).

$$\varepsilon_f = V_{fdo} / V_{sw} \qquad K_f \equiv \frac{-1}{v_f}\frac{\partial v_f}{\partial P}$$

$$\varepsilon_h = 1+V_{hd} / V_{sw} \qquad K_h \equiv \frac{-1}{v_h}\frac{\partial v_h}{\partial P}$$

$$\begin{aligned}
&\Delta P = P_e - P_i \\
&V_{hd} = V_{sw}(\varepsilon_h - 1) \\
&V_{hi} = \varepsilon_h V_{sw} \\
&V_{he} = V_{hi}(1-K_h\Delta P) \\
&V_{sw} = S\pi\phi^2 / 4 \\
&V_{fdo} = \varepsilon_f V_{sw}
\end{aligned} \qquad \text{(A-2)}$$

$$1-\eta_K = \frac{m_i v_{fi}}{V_{sw}} = \frac{v_{fi}}{V_{sw}}\left(\frac{V_c}{v_{fi}} - \frac{V_{fd}}{v_{fe}}\right);\ v_{fe} = v_{fi}(1-K_f\Delta P)$$

$$= \frac{v_{fi}}{V_{sw}}\left(\frac{V_c}{v_{fi}} - \frac{V_{fd}}{v_{fi}(1-K_f\Delta P)}\right) = \frac{V_c}{V_{sw}} - \frac{V_{fd}}{V_{sw}(1-K_f\Delta P)}$$

$$V_c = V_{sw} + V_{fdo} = V_{sw}(1+\varepsilon_f)$$

$$V_{fd} = V_{fdo} + V_{hi}K_h\Delta P = \varepsilon_f V_{sw} + \varepsilon_h V_{sw}K_h\Delta P = V_{sw}(\varepsilon_f + \varepsilon_h K_h \Delta P)$$

$$1-\eta_K = \frac{V_{sw}(1+\varepsilon_f)}{V_{sw}} - \frac{V_{sw}(\varepsilon_f+\varepsilon_h K_h\Delta P)}{V_{sw}(1-K_f\Delta P)} = 1+\varepsilon_f - \frac{\varepsilon_f+\varepsilon_h K_h \Delta P}{1-K_f\Delta P}$$

$$\eta_K = \frac{\Delta P(\varepsilon_f K_f + \varepsilon_h K_h)}{1-K_f\Delta P}$$

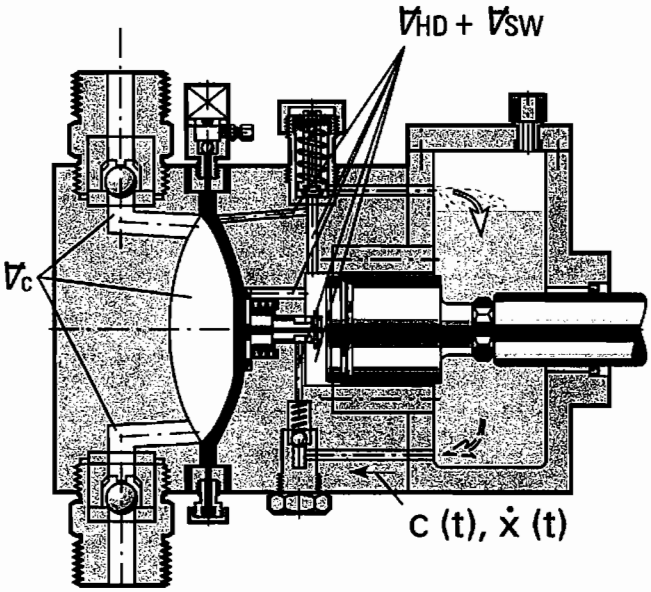

Figure A-10. Schematic of Diaphragm Pump Internals, Positioned at the End of the Suction Stroke (Time, t = 0; Position x = 0).

The head efficiency effect factor, η_G, includes:

- Leakage of the process liquid via backflow through the pump check valves,
- Leakage past the plunger and any valves or seals internal to the pumping chamber, and
- Pump head flexing.

The issue of pump head flexing is complex and, moreover, generally across the industry regarded to be a sufficiently lower order effect as to be ignored. It is assumed to be negligible for purposes here as well. This leaves the various leakage effects that vary according to the size, component design, and condition of the pump. The model for these leakages is that of a restrictive flowpath and hence will vary inversely with the pump speed, i.e., leakage increases with lower pump speed due to the increased time available for leakage to occur. Equationally, this becomes,

$$\eta_G = \left(\eta_{Gp} + \frac{\eta_{Gh}\Delta P}{100}\right)\frac{N_R}{N} \qquad \text{(A-3)}$$

where the leakage components for the product check valves, η_{Gp}, and the internal pump chamber, η_{Gh}, are obtained from the pump manufacturer for each particular application. Hence,

$$\eta_V = 1 - \frac{\Delta P(\varepsilon_f K_f + \varepsilon_h K_h)}{1-K_f\Delta P} - \left(\eta_{Gp} + \frac{\eta_{Gh}\Delta P}{100}\right)\frac{N_R}{N} \qquad \text{(A-4)}$$

ONLINE CHARGING OF GAS-PADDED PULSATION DAMPENERS WHILE RUNNING

As a result of incidents of gas precharge leakage and of inadvertent incorrect precharge, it is recognized that a procedure is necessary to be able to reestablish the correct nitrogen charge in gas-padded pulsation dampeners online without shutting down the pump. To this end the following procedure has been developed.

The recommended *precharge*, β, in a gas-padded pulsation dampener according to various manufacturers varies from 70 to 80 percent. This is the pressure of nitrogen to be applied to the dampener at operating temperature, Tp, but with no pressure on the process side. Thus, in this precharge process, the nitrogen-filled bladder completely occupies the chamber volume, V_d, so that the mass of nitrogen is,

$$m_d = \frac{\beta P_p V_d}{RT_p} \qquad \text{(A-5)}$$

If the dampener is to be recharged online, a procedure is needed to achieve this same mass of nitrogen. A process is proposed here that utilizes a *receiver vessel* with a volume selected for the particular dampener application.

The principle and the apparatus necessary are simple. A tubing tee is connected to the charging valve of the dampener, one side connected through a valve to a nitrogen source and the other through a valve to the *receiver vessel.*

With the receiver valved out, the dampener is first overcharged to a pressure, P_1, above the maximum process pressure, including pressure dynamics. This ensures that the nitrogen within the bladder occupies the entire dampener chamber. Knowing the temperature, pressure, and volume means the mass of nitrogen in the dampener is known to be,

$$m_{dl} = \frac{P_1 V_d}{RT_p} \qquad \text{(A-6)}$$

The valve to the nitrogen source is then closed. The valve is then opened to the receiver, initially at vacuum, atmospheric, or other predetermined pressure, P_r. The pressure equalizes in both the receiver and the dampener at the process operating pressure. Equilibrium temperatures are measured, which enables calculating the initial and final mass of nitrogen in the receiver to be,

$$m_{rl} = \frac{P_r V_r}{RT_{rl}} \qquad \text{(A-7)}$$

$$m_{r2} = \frac{P_p V_r}{RT_{r2}} \qquad \text{(A-8)}$$

Equation (A-8) may alternatively be expressed in the following forms, which will be convenient to use later.

$$V_r = \frac{V_d}{T_p}\left(\frac{P_1 - \beta P_p}{P_p/T_{r2} - P_r/T_{rl}}\right) \qquad \text{(A-9)}$$

$$P_1 = \beta P_p + \frac{V_r T_p}{V_d}\left(\frac{P_p}{T_{r2}} - \frac{P_r}{T_{rl}}\right) \qquad \text{(A-10)}$$

$$P_r = P_p\frac{T_{rl}}{T_{r2}} + \frac{V_d}{V_r}\frac{T_r}{T_p}(\beta P_p - P_1) \qquad \text{(A-11)}$$

To implement this technique, there are three variables to consider.

- The receiver volume, V_r
- The dampener overcharge pressure, P_1, and
- The initial receiver pressure, P_r.

The dampener overcharge pressure, P_1, must not be lower than the maximum mean plus dynamic pressure in the process, (P_{pm} + δP_p), but cannot be higher than the rated pressure of the dampener, P_{dr}. Hence,

$$(P_{pm} + \delta P_p) \le P_1 \le P_{dr} \qquad \text{(A-12)}$$

To size the receiver, Equation (A-9) is used with the overcharge pressure, P_1, replaced by the maximum mean plus dynamic pressure in the process, $(P_{pm} + \delta P_p)$, or:

$$V_r \geq \frac{V_d}{T_p}\left(\frac{P_p(1-\beta)+\delta P_p}{P_p/T_{r2}-P_r/T_{rl}}\right) \quad \text{(A-13)}$$

and the temperatures and pressures evaluated at conditions that maximize the right-hand-side of this equation.

• *Example 2*—A positive displacement plunger pump is equipped with a 2 liter nitrogen gas padded pulsation dampener on discharge with a design pressure of 180 barg. The process and environmental conditions are shown in Table A-1.

Table A-1. Example 2 Process and Environmental Conditions.

	Normal	Maximum	Minimum
Process pressure, barg	152	157	143
Dynamic pressure, bar	18	18	10
Process temperature, °C	110	130	80
Ambient temperature, °C	17	33	0

What should be the volume of a receiver to be used in an online charging procedure as outlined in Table A-1?

• *Solution*—To size this receiver, the minimum size should be evaluated. Assume the initial receiver pressure to be atmospheric. Utilizing Equation (A-13) with variables chosen to maximize the right-hand-side,

$$V_r = \frac{2}{273+80}\left(\frac{(157+1)(1-0.7)+18}{(157+1)/273-1/273}\right) = 32.2\% \text{ of } 2\text{l} = 0.64\text{ l} \quad \text{(A-14)}$$

To provide a small margin on size, perhaps the receiver volume should be 0.75 liter.

• *Example 3*—For the positive displacement plunger pump, dampener, and receiver of *Example 2*, determine the charge pressure, P_1, to be used if the process and environmental conditions at a point in time are as follows.

β = 0.8
T_p = 80°C
P_p = 157 barg
$T_{rl} = T_{r2}$ = 33°C
δP_p = 18 bar

• *Solution*—Assuming the reservoir initially at one atmosphere and applying Equation (A-12),

$$P_1 = 0.8(157+1)+\frac{0.75(273+80)}{2}\left(\frac{157+1}{273+33}+\frac{1}{273+33}\right) = 213 \text{ bara} \quad \text{(A-15)}$$

But this overcharge pressure exceeds the design pressure of the dampener. Hence it is necessary to initially charge the receiver above atmospheric pressure. If the dampener overcharge, P_1, is arbitrarily set to the design pressure of 180 barg, then Equation (A-11) may be used to determine the necessary receiver precharge as,

$$P_r = 157+\frac{2}{0.75}\left(\frac{273+33}{273+80}\right)[0.8(158)-181] = 30.8 \text{ barg} \quad \text{(A-16)}$$

Hence, the 0.75 liter receiver should be precharged to 30.8 barg. The pulsation dampener should then be overcharged to 180 barg. Carrying out the above procedure then will result in producing the desired dampener effectiveness in operation.

SIMPLE GUIDELINES IN THE DESIGN OF PIPING WITH REGARD TO PRESSURE PULSATION

Dynamic flow and pressure, or *pulsation*, are always a concern in a positive displacement pumping system. Approaches to dealing with pulsation in design can range from doing nothing to hiring a rigorous study using computer simulation. Intermediate approaches include applying rule-of-thumb sizing for pulsation dampeners oneself and relying upon pump or pulsation dampener vendors to make recommendations. Unfortunately, the user or owner often sees the entire matter as mysterious and lacks a basis upon which to decide how to address pulsation. While there are no quick answers or rules, the purpose of this section is to provide some basic guidelines on how to estimate the fundamental and other low-order acoustic natural frequencies at least in those systems that lend themselves to simplistic representation. These can then be compared with the pulsation frequencies emitted by the pump, which might therefore cause problems warranting a more detailed analysis. These same guidelines applied to an existing system displaying high vibration, suspected to be caused by pulsation, may provide insight into the nature of that dynamic behavior. This, in turn, may be helpful in evaluating alternative solutions.

Consider the system shown in Figure A-11. While no real system is ever this simple, it may be possible to approximate this by ignoring small and short branch connections, and if most of the flow is from "point A to point B." Even heat exchangers can usually be approximated by a line of the same length as the total internal flowpath. To the extent, however, that there is significant branching, flow restrictions and sudden pressure drops, large changes in flow velocity, intermediate volumes, etc., this type of approximation becomes too inaccurate to be useful.

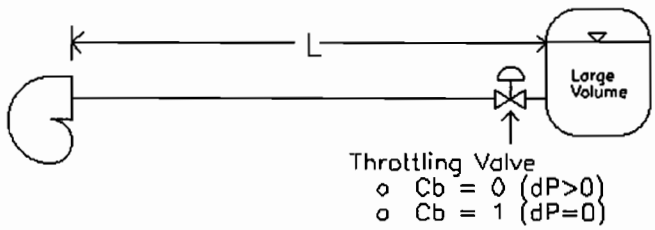

(a) System with NO Pulsation Dampeners

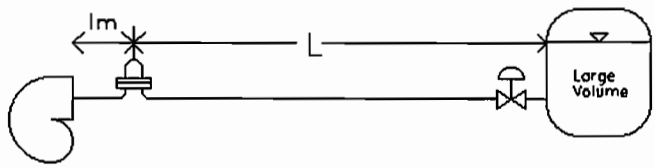

(b) System WITH Pulsation Dampener

Figure A-11. Simplified Piping System for Approximating Pressure Pulsation Characteristics.

The fundamental pipe mode natural frequencies in the Figure A-11 model are primarily a function of only three parameters.

• Overall length, L

• Sonic velocity, a, of the liquid flowing in the pipe

• The boundary condition, C_b, at the end of the pipe away from the pump

Only two boundary conditions are treated here (Figure A-11).

• $C_b = 0$ —Line terminates in a throttling valve, spray bar, or other element with significant pressure drop

• $C_b = 1$—Line termination in a large capacitive tank with minor or no discrete pressure drop additional to nominal entrance loss

The low-order acoustic natural frequencies are given approximately by,

$$f_{ni} \approx (2i - C_b)\frac{a}{4L}; \; i = 1,2,3,... \qquad \text{(A-17)}$$

• *Example 4*—The pump from *Example 3* discharges to the piping system shown in Figure 30. The normal operating speed range of the pump is 120 to 180 rpm. Determine whether acoustic natural frequencies might be expected to be excited by the pump and at near which pump speeds.

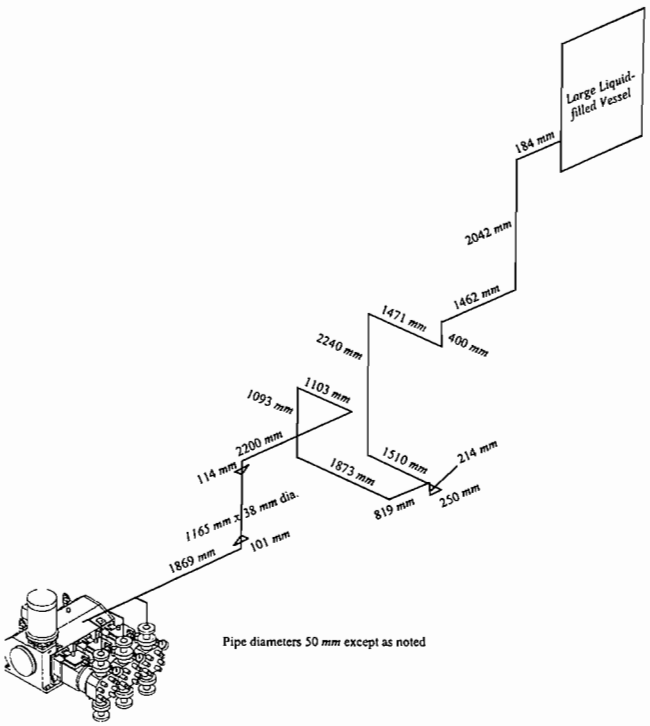

Figure A-12. Isometric of Actual Pump Discharge Piping System for Example 4 Evaluation of Acoustic Frequency Response Characteristics.

• *Solution*—Ignore the cross-section change in the 1165 mm span and simply approximate the entire length of the pipe to be the flow distance from the middle pump head to the downstream pressure vessel. Therefore,

L ≈ 23 m
a = 1390 m/s
C_b = 1

Hence, from Equation (A-17),

$$f_{ni}, Hz \approx 13,39,65,91,...; \; i = 1,2,3,4,... \qquad \text{(A-18)}$$

In terms of exciting one or more of these, the most probable and most severe would be expected near a running speed of about 130 rpm. The base excitation frequency for the three-head pump would be 6.5 Hz and twice this base frequency would correspond to the 13 Hz acoustic natural frequency.

For comparison of these results with a method of greater accuracy, a rigorous analysis of the exact system of Figure A-12 was performed with a digital computer simulation program. The calculation method and additional details of this program are beyond the scope of this paper. Figure A-13 shows the frequency response for this analysis for a point near the pump discharge, which indicates the errors introduced by the above approximation method to be on the order of about 10 percent. Figure A-14 shows the "mode shapes" of pressure and flow pulsation for the modes at 11, 33, and 59 Hz. This type of illustration is useful to help in understanding where the nodes and antinodes of pulsation physically are located along the length of the pipeline.

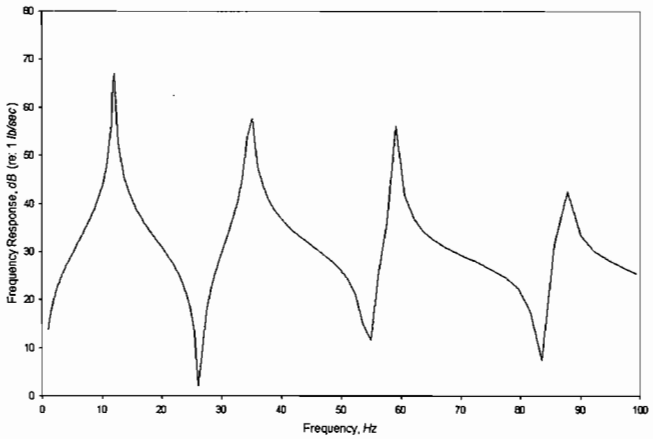

Figure A-13. Acoustic Frequency Response for a Point Near Pump Discharge.

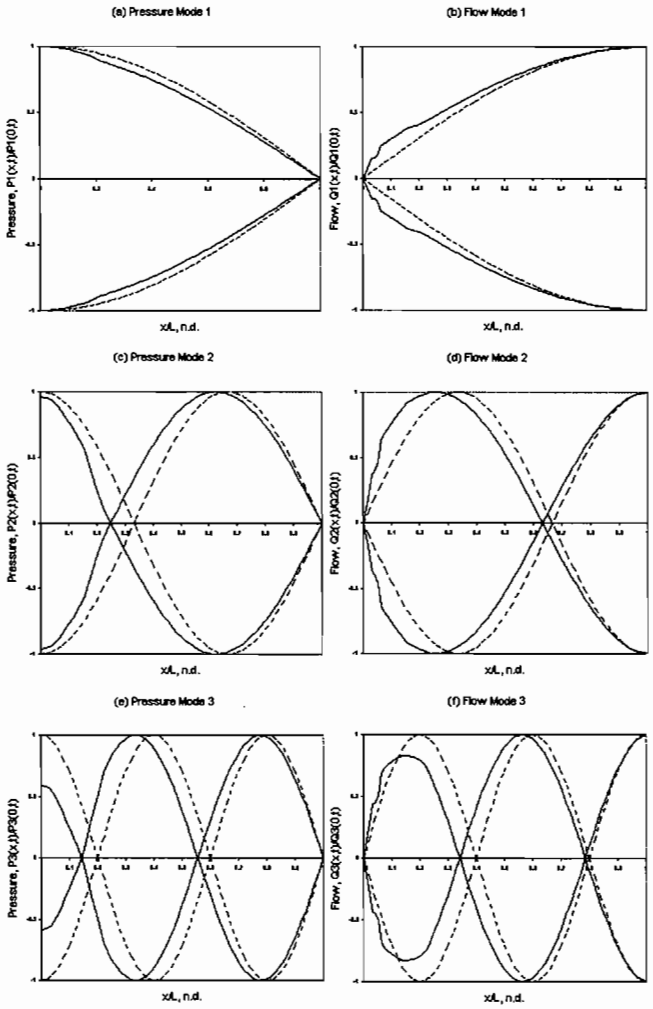

Figure A-14. Modes Shape Envelopes for Modes 1, 2, and 3 of Example 4, Comparison of Higher-Order Pulsation Analysis (solid bold lines) with Simplified Approximation (dashed lines).

It is worth reiterating that as an actual system becomes more complex versus the Figure A-11 simple approximation, the error in Equation (A-17) increases. Hence, care should always be excercised in applying this equation.

• *Example 5*—The pump and piping system of *Example 4* is modified such that the discharge is through a spray bar into a nominal atmospheric gas space instead of into a pressurized liquid volume. Estimate the acoustic natural frequencies.

• *Solution*—Applying Equation (A-17) with the boundary condition parameter, $C_b = 0$, yields,

$$f_{ni},Hz \approx 26,52,78,...; \; i = 1,2,3,4,... \qquad (A\text{-}19)$$

Figure A-15 shows the frequency response near the pump analyzed with the rigorous digital simulation. The error introduced by Equation (A-19) is again shown to be on the order of 10 percent.

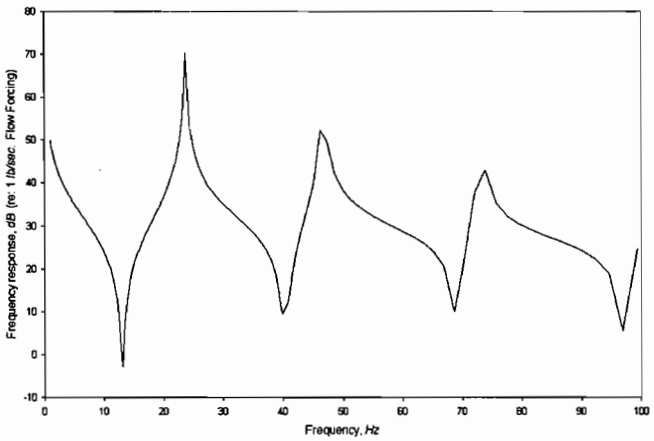

Figure A-15. Acoustic Frequency Response for a Point Near Pump Discharge.

Figure A-16 shows the mode shapes of pressure and flow pulsation for the first three low-order acoustic natural frequencies. Notice that these modes and frequencies differ from those in *Example 4* due to the effect of the downstream boundary condition. This difference in boundary condition means that natural frequencies, or antinodes of pulsation, in the *Example 4* system are very nearly nodes, or frequencies of minimum vibration, in the *Example 5* system, and vice versa. This is seen clearly in comparing Figures A-14 and A-16.

REFERENCES

Joukowsky, N., 1898, "About the Hydraulic Impact in Water Pipelines," Petersburg, Russia.

Schlücker, E., Blanding, J. M., and Murray, J. F., 1999, "Guidelines to Maximize Reliability and Minimize Risk in Plants Using High Pressure Process Diaphragm Pumps," *Proceedings of the Sixteenth International Pump Users Symposium*, Turbomachinery Laboratory, Texas A&M University, College Station, Texas, pp. 77-100.

Schlücker, E., Strizelberger, M., Fritsch, H., and Schwarz, J., 1997, "A New Method for Estimating NPSH Values of Reciprocating Positive Displacement Pumps," ASME Fluids Engineering Division Summer Meeting, Vancouver, British Columbia.

Vetter, G., Schlücker, E., and Horn, W., 1994, "Diaphragm Development Trends for Safe Leakfree Reciprocating Process Pumps," *Proceedings of the Twelfth International Pump Users Symposium*, Turbomachinery Laboratory, Texas A&M University, College Station, Texas, pp. 207-220.

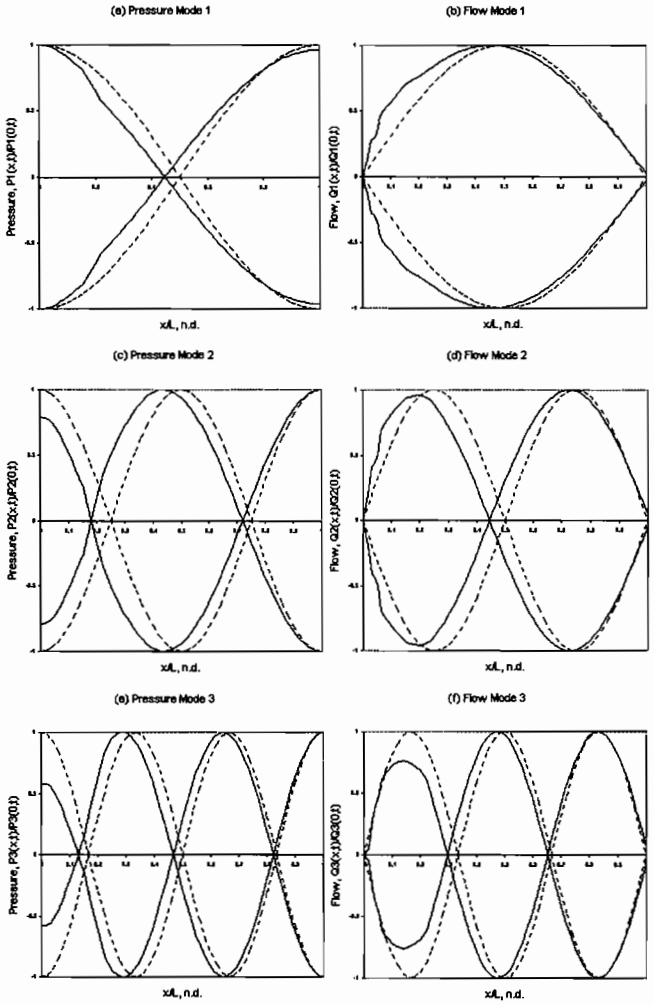

Figure A-16. Modes Shape Envelopes for Modes 1, 2, and 3 of Example 5, Comparison of Higher-Order Pulsation Analysis (solid bold lines) with Simplified Approximation (dashed lines).

BIBLIOGRAPHY

Schlücker, E. and Horn, W., 1996, "High Pressure Process Pump Application and Technical Requirements," Third International Symposium on High Pressure Chemical Engineering, Zurich, Switzerland, Elsevier Verlag Amsterdam, Lausanne, New York.

ACKNOWLEDGEMENT

The authors wish to acknowledge individuals and organizations whose contributions have made this work possible.

Robert J. Hart, former Principle Consultant with DuPont Company, now an independent consultant, has provided considerable assistance in many aspects of the design of pumping systems including, among many other areas, the setting of operating, relief, and design pressures.

David M. Mellen, Engineering Fellow, DuPont Company, has pioneered and developed monitoring systems within DuPont for many years including the systems in use today that form the basis for the capabilities and learnings, and conclusions comprising the current work.

Josef Schwarz and Marcus Sachse, LEWA, have contributed methodologies and calculation methods in many areas including the Joukowsky Shock Effect in the context of product check valve actuation in positive displacement pumps, volumetric efficiency, and in other areas.

The LEWA company made available the test pump in Leonberg, Germany, with instrumentation and resources to carry out the

controlled experimental testing for normal and specific fault condition abnormal operation, which was fundamentally important in the current work.

The Lycra™ THF business at DuPont has provided many hardware, software, and personnel resources that have made this work possible.